DOE/PC/79913-T9

AERATED ATOMIZATION OF COAL WATER SLURRY

DOE/PC/79913--T9

DE91 001311

Report prepared by
Harry N. Buckner, Paul E. Sojka, and Arthur H. Lefebvre

for
DOE/PETC, Pittsburgh

under
Grant No. DE-FG22-87PC79913

Contract Monitor: Mr. Anthony Mayne

January 5, ~~1988~~ 1989

Thermal Science and Propulsion Laboratory
School of Mechanical Engineering
Purdue University, West Lafayette, IN 47907

INTRODUCTION

A photographic study of the flow field within the nozzle and the spray has been made to further analyze the atomization process. The photographs were made at the nozzle, and 38mm, 100mm, 150mm, 250mm, and 275mm downstream of the nozzle exit. Results show the quality of atomization at different air liquid ratios (ALR) and, more importantly, how ALR influences the flow field. The development and structure of the drops is also illustrated.

ATOMIZATION

In the previous report, photographs of the atomization process are presented, and in them, quality atomization is shown to exist when the nozzle operates in the annular, wispy, and slug flow regimes. Close inspection of these photographs reveals micro-bubbles, on the order of 50 microns in diameter, suspended in the fluid. Further analysis and observation of this phenomenon has been made in order to determine the effect of these micro-bubbles on the atomization process.

In order to observe the consequences of the micro-bubbles, the ALR was increased from 0.0 to 0.35. When the ALR was 0.0, the liquid jet showed no sign of instability, containing no ripples, waves, or surface discontinuities (see figures 1-4). With the addition of a small amount of air (ALR = 0.0064), two distinct size classes of bubbles formed. The larger bubbles (length approximately 10 mm) were termed macro-bubbles and the smaller bubbles (approximately 50 microns in diameter) were termed micro-bubbles. Macro-bubbles resulted in flow transition to slug flow (see figures 5-8). The slugs did not break up upon exiting the nozzle. Note that the exiting liquid resembles a froth because of micro-bubbles being in suspension. While slugs do not break up upon exit, expansion of macro-bubbles, located between slugs, leads to formation of satellite drops (figure 9). These satellite drops also contain micro-bubbles. The data taken suggests that micro-bubbles do not explode upon exiting the nozzle.

Photographs taken while spraying pure glycerin (k=1400, n=0.97) show no transition between bubbly flow and slug flow (figures 10-13). This gives further evidence that aerated atomization will not be possible when using highly viscous fluids.

The initial discovery of the micro-bubbles was made while spraying pure glycerin. In order to gain more understanding of the effect of these bubbles, photographs were taken when atomizing lower viscosity fluids. It was discovered that as viscosity decreased, the micro-bubbles, seen in figures 14 and 15, eventually disappeared, as shown in figure 16. This indicates that the high viscosity liquids are able to capture and retain small amounts of air while the lower viscosity fluids are not able to keep the air in suspension. This suggests micro-bubbles may in some cases have insufficient buoyancy to overcome the viscous forces in the liquid.

The breakup and development of drops was also investigated photographically. Photographs taken 75mm to 100mm downstream of the nozzle exit show ligaments are formed in the initial breakup of fluids. These ligaments later develop into drops (figure 17). Photographs were taken 150mm and 275mm downstream of the nozzle exit to determine the point at which drops were formed. These photographs showed, that in the majority of cases, the ligaments had formed into drops 150mm downstream of the exit. The only exception was the highest viscosity liquid, who's ligaments had developed into drops 250mm downstream.

FUTURE WORK

A more extensive study of the break-up action caused by both bubble size classes is being undertaken. Since operating pressures are as high as 2.2 MPa, it is probable that the air in the bubbles expands at sonic speeds at the nozzle exit. If this is so, then this process can not be subjected to existing theoretical analyses. Our objective then is to develop a theoretical expression that can correlate the data.

A parallel experimental study will employ a microphone and spectrum analyzer to record pressure waves caused by the expanding macro-bubbles. The frequency spectrum will be compared with the rate at which macro-bubbles exit the nozzle. This will indicate the extent to which the pressurized air within the bubbles is influencing the break-up of the liquid. In addition, schlieren photographs will show whether these pressure waves are shock fronts.

SUMMARY

The photographic study revealed the existence of two types of bubbles in the flow field. When atomizing high viscosity fluids micro-bubbles were found suspended in the liquid and remained in this state throughout the atomization process. Macro-bubbles coexisted with the micro-bubbles within the nozzle, but upon reaching the nozzle exit, they burst causing the liquid jet to disintegrate.

The fluid at the nozzle exit was drawn into ligaments as it exited the nozzle. These ligaments later formed droplets. Both ligaments and droplets were filled with the micro-bubbles causing them to resemble a froth. There is no evidence that the micro-bubbles exploded or caused the fluid to break into smaller droplets.

Future analysis will focus on the flow structure at the nozzle exit. By using acoustical techniques and schlieren photographs, measurement of pressure waves at the nozzle exit will be made to determine if shock fronts exist. The explosive nature of the macro-bubbles can then be assessed.

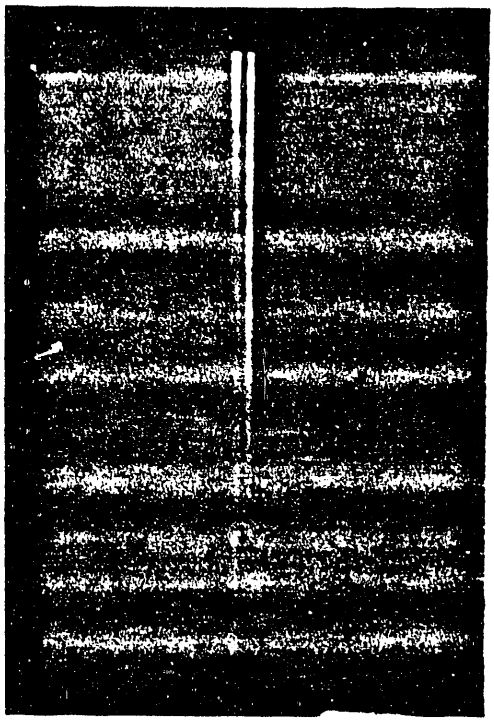

Figure 1: k = 1300, n = 0.97,
ALR = 0.0, 150 mm downstream.

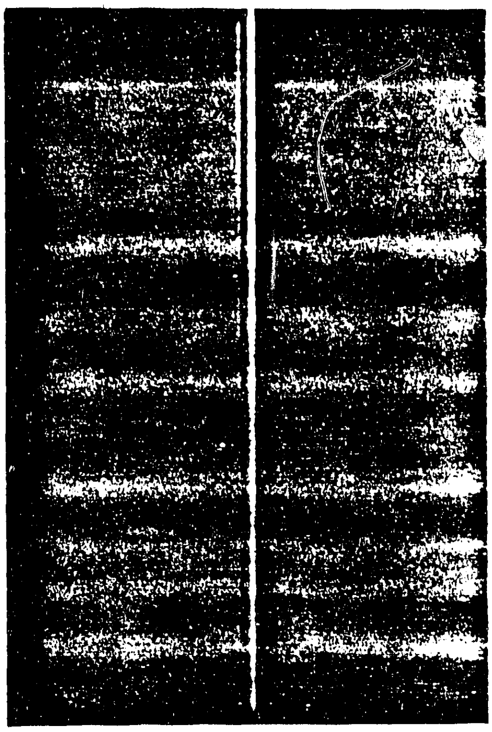

Figure 2: k = 1200, n = 0.97,
ALR = 0.0, 275 mm downstream.

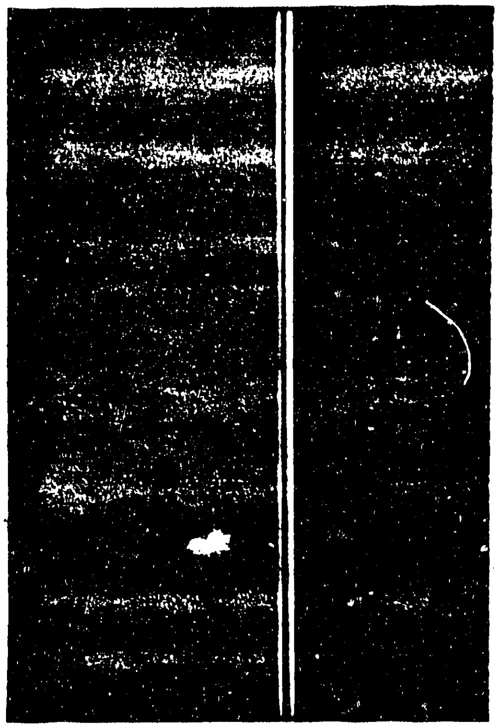

Figure 3: k = 80, n = 0.96,
ALR = 0.0, 275 mm downstream.

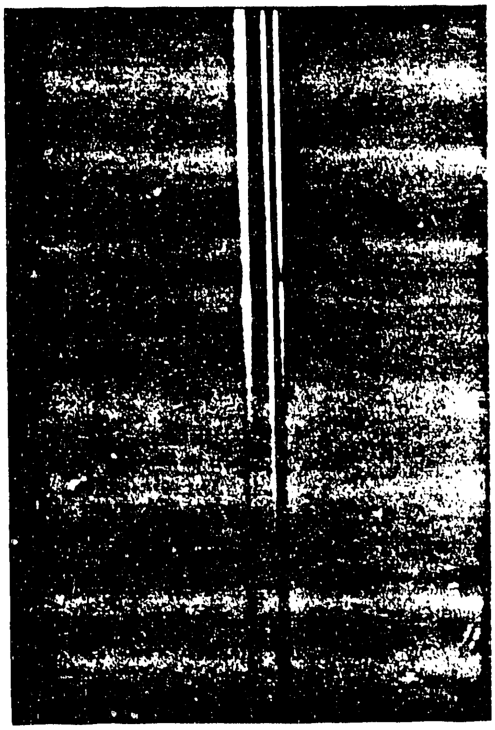

Figure 4: k = 530, n = 0.97,
ALR = 0.0, 250 mm downstream.

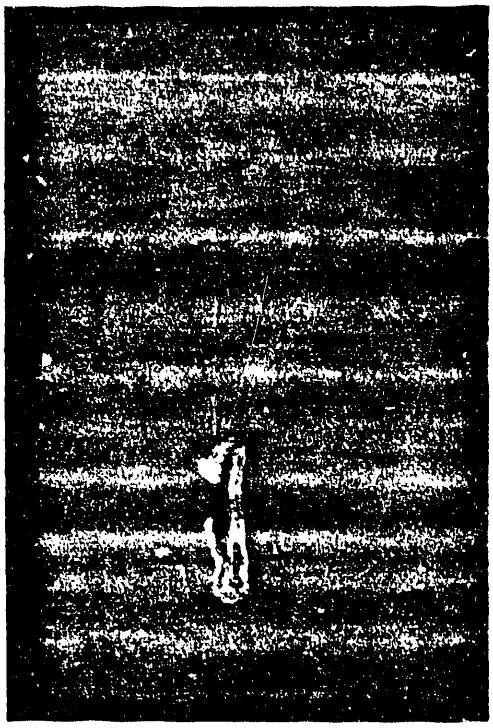

Figure 5: k = 1500, n = 0.97, ALR = 0.0064, 150 mm downstream.

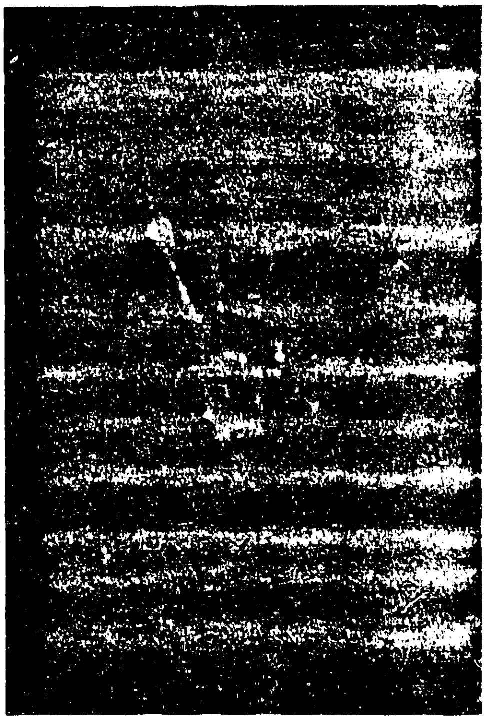

Figure 6: k = 1500, n = 0.97, ALR = 0.0064, 250 mm downstream.

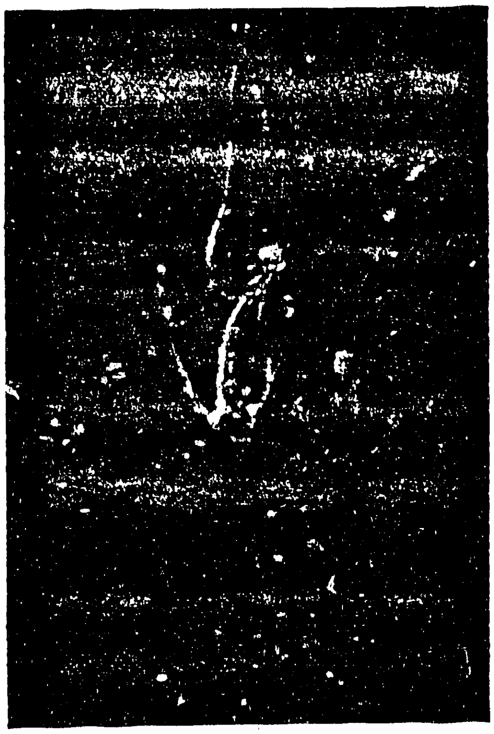

Figure 7: k = 530, n = 0.97, ALR = 0.0064, 150 mm downstream.

Figure 8: k = 80, n = 0.96, ALR = 0.0064, 150 mm downstream.

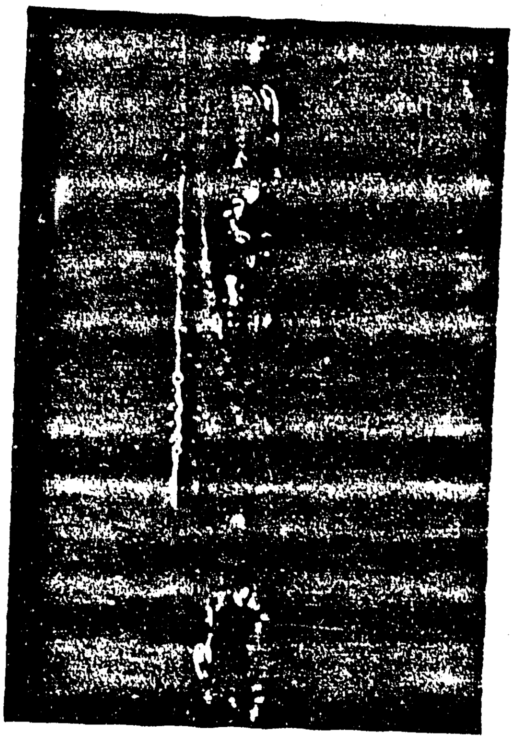

Figure 9: k = 1400, n = 0.97, ALR = .0098, at nozzle.

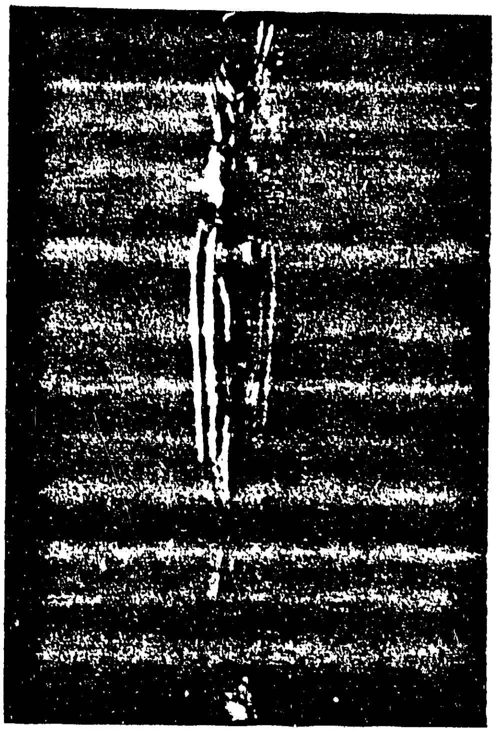

Figure 10: k = 1500, n = 0.97, ALR = .0064, at nozzle.

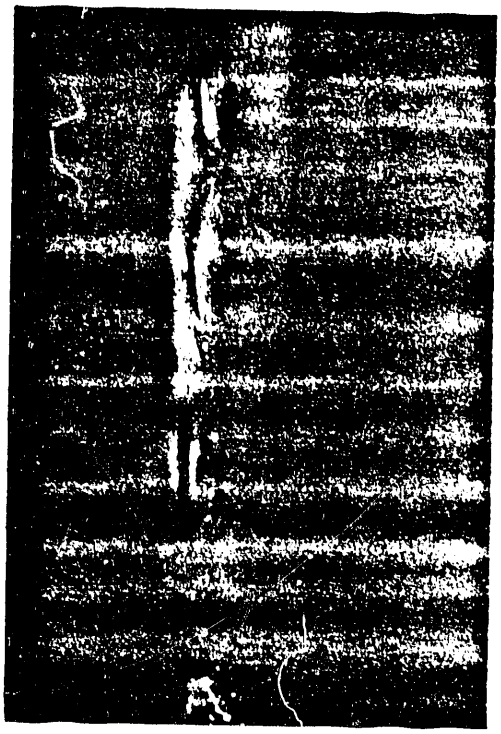

Figure 11: k = 1500, n = 0.97, ALR = .0839, at nozzle.

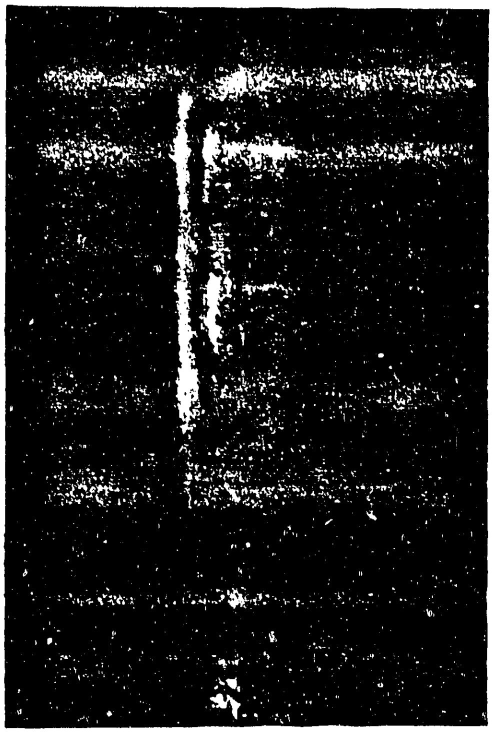

Figure 12: k = 1500, n = 0.97, ALR = .1613, at nozzle.

Figure 13: k = 1500, n = 0.97, ALR = .3534, at nozzle.

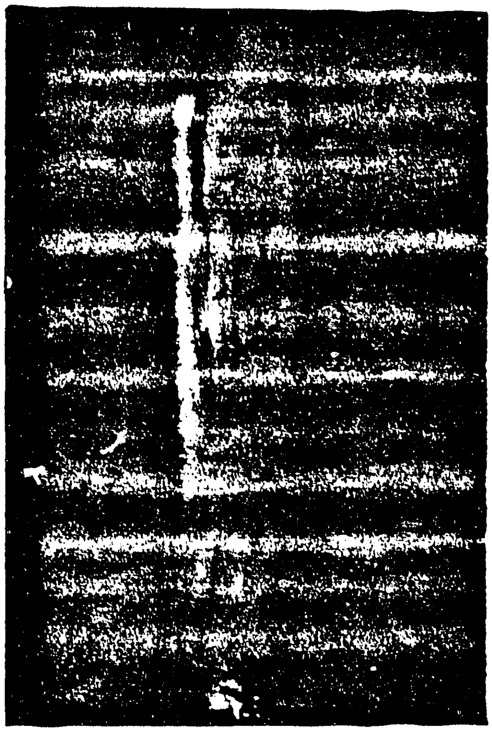

Figure 14: k = 1500, n = 0.97, ALR = 0.1613, at nozzle.

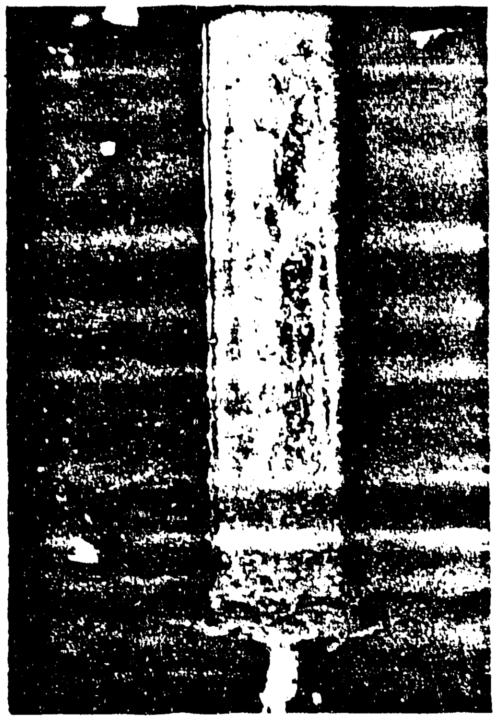

Figure 15: k = 530, n = 0.97, ALR = 0.1613, at nozzle.

Figure 16: k = 80, n = 0.96, ALR = 0.1613, at nozzle.

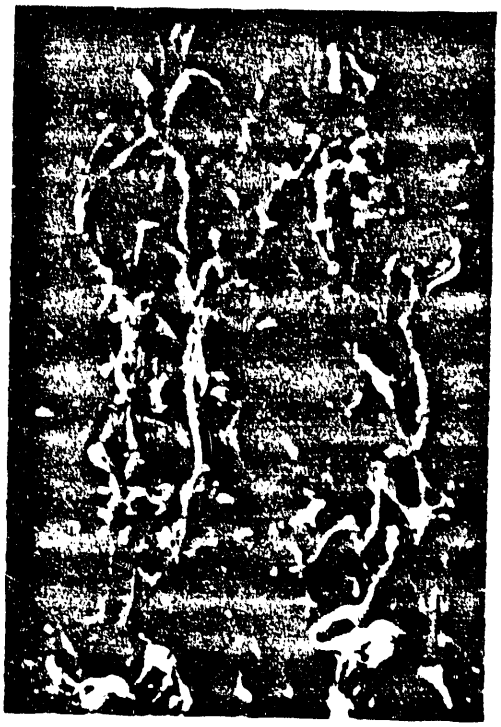

Figure 17: k = 1200, n = 0.97, ALR = .0839, 38mm downstream.

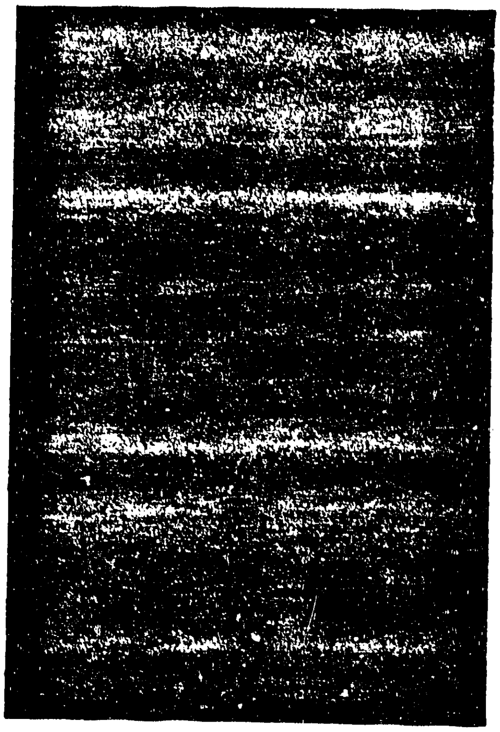

Figure 18: k = 1200, n = 0.97, ALR = 0.1613, 275mm downstream.

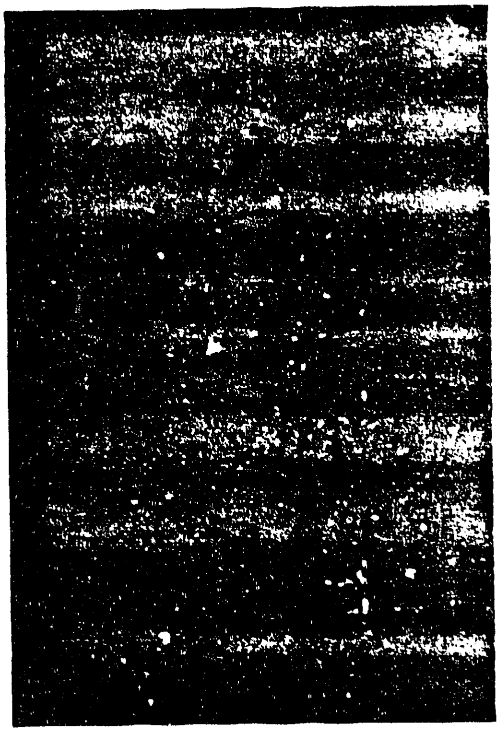

Figure 19: k = 1500, n = 0.97, ALR = 0.0839, 150mm downstream.

- END -

DATE FILMED

11 / 20 / 90